Materials Transactions, Vol. 45, No. 2 (2004) pp. 315 to 318

Visualization of Hydrogen Distribution in Tensile-Deformed Al-5%Mg Alloy Investigated by means of Hydrogen Microprint Technique with EBSP Analysis*1

Keitaro Horikawa*2 and Kenichi Yoshida

Department of Mechanical Engineering, Faculty of Engineering, The University of Tokushima, Tokushima 770-8506, Japan

Hydrogen distribution in high-purity-based polycrystalline Al-5%Mg alloys prepared by changing the melting atmosphere was visualized by means of hydrogen microprint technique with electron backscattering pattern analysis after a tensile deformation at room temperature. The number of hydrogen atoms observed as silver particles on the slip lines was increased when the applied strain was increased. Hydrogen atom observed on the slip lines was totally increased when the melting atmosphere of the alloys was changed from argon to air. Hydrogen atom was observed at both slip lines and special grain boundaries when an air-melted specimen was deformed. It was shown that hydrogen atom accumulation at grain boundaries varied with the misorientation of grains and the angle to the tensile direction.

(Received November 7, 2003; Accepted December 19, 2003)

Keywords: *aluminum alloy, hydrogen, grain boundary, slip line, deformation*

1. Introduction

Solid solution hardenable 5000 series aluminum alloys of Al-Mg based are widely used as an engineering material since they have good formability and high corrosion resistance. However, a polycrystalline Al-5%Mg alloy with a coarse grain size of 300 μm is reported to show decrease in ductility at room temperature[1] and at high temperatures around 300°C[2–5] when it contains high amounts of hydrogen introduced from the melting and casting atmospheres. This phenomenon is believed to be a kind of hydrogen embrittlement (HE) of this alloy. Itoh *et al.*[1] have shown that the amount of hydrogen evolved at the moment of fracture was increased when an Al-5%Mg alloy was melted in air and tensile tested at room temperature compared with an Al-5%Mg alloy melted in argon. They concluded that hydrogen would accelerate the nucleation of transgranular voids which were formed under triaxial tensile stress after necking. For the explanation of such hydrogen related transgranular fracture, the mechanism of hydrogen enhanced localized plasticity has been proposed on the basis of experimental observations and theoretical calculations.[6–11] On the other hand, Okada and Kanno[5] reported that an Al-5%Mg alloy melted in air showed severe intergranular fracture when tested around 300°C and that 0.04 mass% of additional yttrium was capable of suppressing the intergranular fracture, where yttrium bearing compounds trapped the hydrogen. The effect of melting atmospheres and additional elements on HE was investigated using a testing machine consisting of a quadrupole mass spectrometer and an ultrahigh vacuum chamber.[1,4] However, distribution of hydrogen in grain interiors and grain boundaries during the tensile deformation has not been fully examined on the basis of microscopic observation. In this study, high-purity-based Al-5%Mg alloys were prepared by changing the melting atmosphere and then hydrogen evolution to the specimen surface accompanied by the deformation was visualized by means of a hydrogen microprint technique (HMT), which is known as one of the hydrogen visualizing methods using the redox reaction between hydrogen and silver bromide.[12] An electron backscattered pattern (EBSP) analysis was also performed for the specimens applied HMT to elucidate the relationship between the accumulation of hydrogen and the orientation of grains.

2. Experimental Procedure

High-purity aluminum of 99.999 mass% purity, magnesium of 99.98 mass% purity, and a crucible made of electrode grade graphite were used in the same way as in the authors' previous papers[3,4] to eliminate the effect of other impurities than hydrogen (for simplicity, "mass%" is expressed as "%" below). Two kinds of Al-5%Mg binary alloy were melted in air or argon and cast into an iron mold. Magnesium content was 4.9% in the air-melted alloy and 5.1% in the argon-melted one. Maximum impurity contained in the alloys was 0.0035% silicon. For the melting in argon, argon was introduced into a closed chamber after melting pure aluminum in a vacuum of about 5×10^{-3} Pa in the same manner as previously reported.[3,4] Alloy ingots were homogenized at 430°C for 18 h in the argon atmosphere and subsequently cold-rolled by 70%. Plate test pieces 10 mm in gage length, 5 mm in width and 1 mm in thickness were machined by electro-discharge machining from the rolled sheets, and then annealed at 510°C for 0.5 h in a furnace to get a coarse grain size of about 300 μm.

Before HMT testing, surfaces of the specimens were mechanically polished and then electropolished to remove the strained layer, and orientation of individual grains was measured by EBSP in a scanning electron microscope (SEM). The specimen surfaces were covered with a nuclear emulsion (Ilford L-4, diluted 2 times) containing gelatin and silver bromide particles 0.011 μm in size by the wire loop method. Tensile tests were carried out in a dark room at room temperature at an initial strain rate of 8.4×10^{-4} s^{-1}. After the tests, the specimens were kept at room temperature for 30 min, immersed in formalin (40% HCHO water solution) for 30 s to harden the gelatin with a view to preventing

*1This Paper was Presented at the Autumn Meeting of the Japan Institute of Metals, held in Sapporo, on October 13, 2003.

*2Present address: Osaka University, Toyonaka 560-8531, Japan

redistribution of silver particles in the nuclear emulsion, fixed using a $Na_2S_2O_3$ aqueous solution for 3 min and dried in air. Observation of silver particles was performed with an SEM equipped with an energy dispersive X-ray spectrometer (EDXS).

3. Results and Discussion

3.1 Tensile properties and HMT

Tensile properties of the two specimens tested at room temperature are shown in Fig. 1. Elongation and tensile strength were both lowered when the melting atmosphere was changed from argon to air, as reported by Itoh *et al.*[1] Thus, the decrease in ductility would be due to the difference in the hydrogen content. The HMT testing on the fractured specimens revealed that spherical particles were preferentially observed on the multiple slip lines near the fracture points in both specimens as shown in Fig. 2. The particles observed on the slip lines were identified as silver particles by

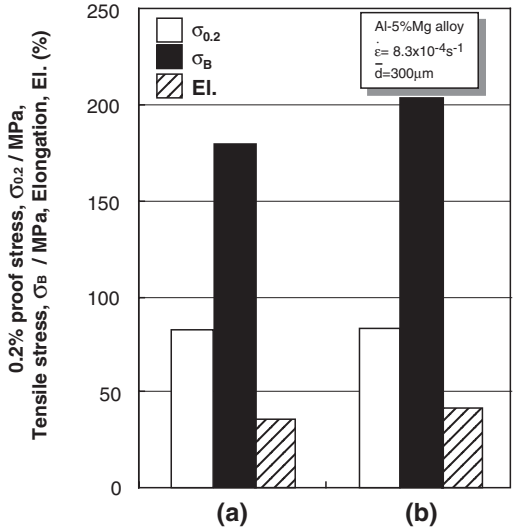

Fig. 1 Tensile properties tested at room temperature in the two alloy specimens prepared in the atmosphere of air (a) or argon (b).

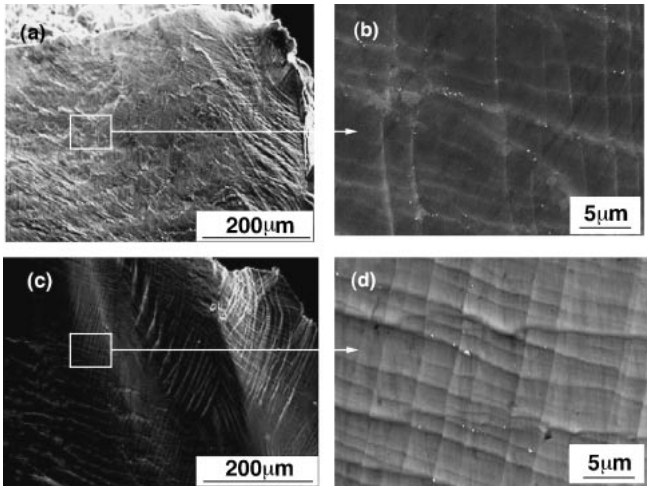

Fig. 2 SEM images showing the particles on slip lines near the fracture point in the two specimens prepared in the atmosphere of air (a), (b) and argon (c), (d).

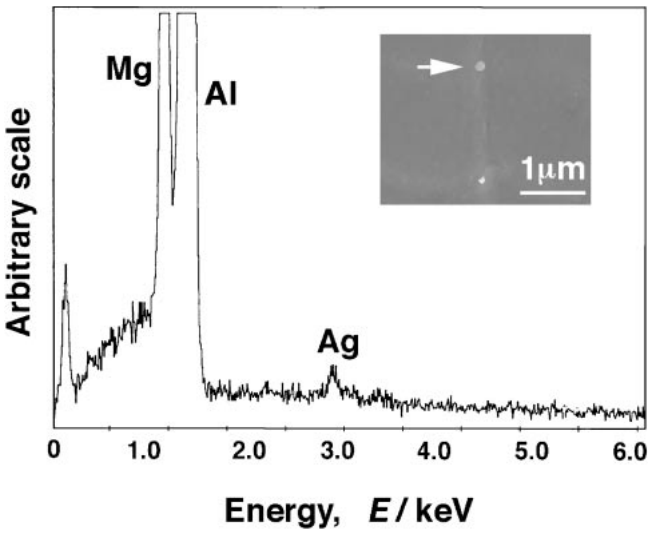

Fig. 3 An SEM image and the result of EDX analysis on a particle on the slip line in the air-melted specimen near the fracture point.

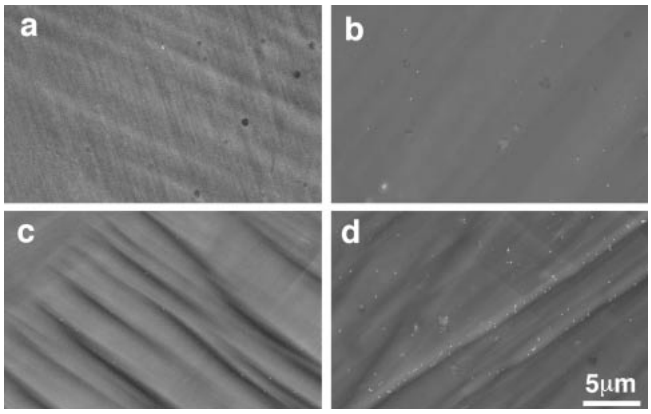

Fig. 4 SEM images showing silver particles on slip lines in the air-melted specimen deformed by 5% (a), 10% (b), 15% (c) and 20% (d).

EDXS analysis as shown in Fig. 3. This array of siver particles cannot be interpreted in terms of pipe diffusion because the time interval between the tensile test and the fixing was so short (30 min). Particle density in the air-melted specimen (Fig. 2(b)) was higher than that in the argon-melted specimen (Fig. 2(d)). This was also in good agreement with the result previously reported by Itoh *et al.*[1] showing that higher amounts of hydrogen were evolved at the moment of fracture in the air-melted Al-Mg alloy than in the argon-melted one. Figure 4 shows the HMT image depending on the applied strain in the air-melted specimen. The number of silver particles observed on the specimen surface was increased with increase in the applied strain. These particles were also clearly visible on the slip lines especially when the applied strain exceeded 20%, while no particles were visible in the undeformed specimen. Thus, it is reasonable to assume that hydrogen is transported to the specimen surface with the aid of mobile dislocations due to the deformation.

3.2 HMT with EBSP analysis

The HMT testing revealed that silver particles were also observed at some special grain boundaries as well as on the

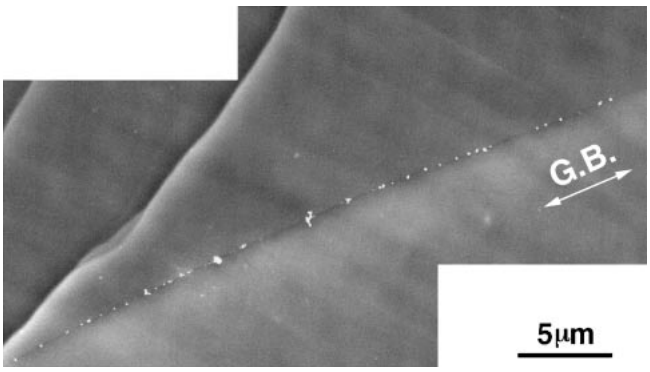

Fig. 5 Silver particles accumulating at a twist grain boundary in the air-melted specimen deformed by 20%.

slip lines. The degree of accumulation of these particles at grain boundaries was shown to be different from the character of the boundaries; many silver particles were accumulated in some grain boundaries, while none were present in other boundaries. Figure 5 shows a result obtained by HMT showing the silver particles accumulating at the grain boundaries after the deformation by 20%. These particles were arranged at the grain boundary maintaining a distance corresponding to the intersection of the slip lines with the boundary. This also suggests that hydrogen is transported to the grain boundary utilizing the slip lines with the aid of mobile dislocation. Comparison of the EBSP map and the SEM image in Fig. 6 showed that the grain boundary in Fig. 5 was a twist boundary; it had a misorientation angle of about 30° around the common rotating axis. The grain

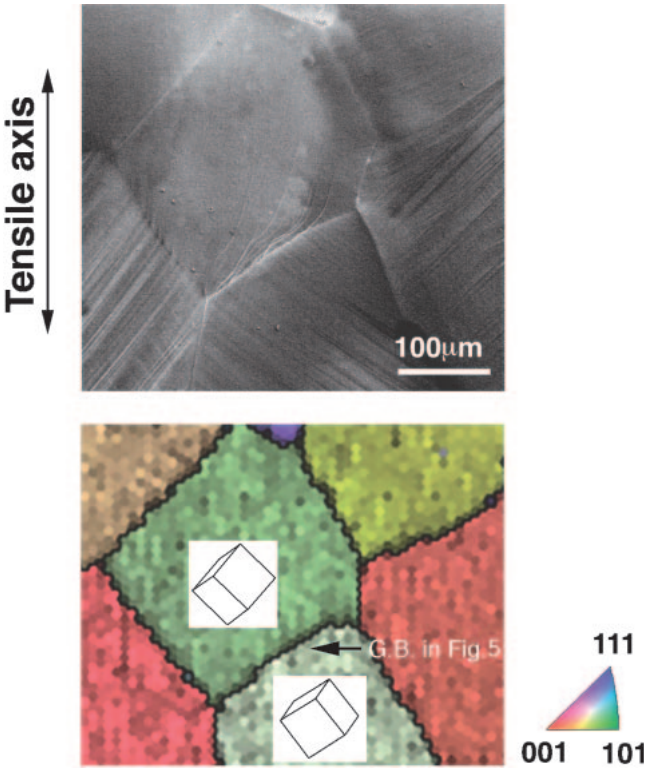

Fig. 6 Relationship between an SEM image and the grain boundary misorientation in the same region as Fig. 5.

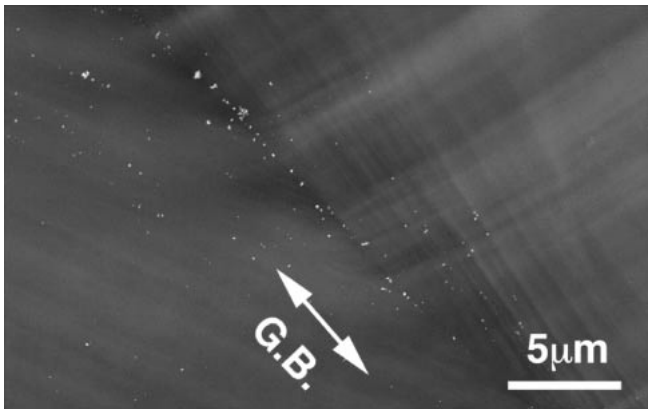

Fig. 7 Silver particles accumulating at a tilt grain boundary in the air-melted specimen deformed by 20%.

interior near the grain boundary (Fig. 6(a)) showed a feature suggesting that a high shear stress was imposed against the boundary. Except for the grain boundary shown in Fig. 5, however, no clear accumulation of silver particles was observed in the other grain boundaries shown in Fig. 6(a). Preferential accumulation of silver particles was also observed in another grain boundary as shown in Fig. 7. In contrast to the results indicated in Figs. 5 and 6, the grain boundary shown in Fig. 7 was a tilt boundary having a misorientation angle of about 20° around the common rotating axis, and numerous slip lines with silver particles were visible near this boundary. No clear shear morphology was identified in the grain interior, however. Based on these two cases, there appears to be a correlation between the slip mode in grain interiors and the accumulation of hydrogen at the grain boundary, as well as the grain boundary misorientation.

4. Summary

Hydrogen in tensile-deformed Al-5%Mg alloys was visualized with HMT combined with EBSP. The results obtained are summarized as follows: (1) The number of silver particles representing hydrogen on the slip bands increased when the melting atmosphere of the alloy was changed from argon to air. (2) Silver particles are accumulated at both slip lines and grain boundaries as the deformation proceeded above 20% in the air-melted alloy. (3) Accumulation of hydrogen at a grain boundary would be different from the slip mode in grain interiors and the grain boundary misorientation.

Acknowledgements

The authors are grateful to Furukawa Electric Co., Ltd. for the analyses of impurities in the Al-Mg alloys. They are also grateful to Prof. M. Kanno and Mr. K. Ichitani for technical support in the HMT testing.

REFERENCES

1) G. Itoh, T. Jinkoji, M. Kanno and K. Koyama: Mater. Trans. A **28** (1997) 2291–2295.

2) G. Itoh, H. Suzuki and K. Koyama: J. JILM **35** (1985) 501–504.
3) K. Horikawa, S. Kuramoto and M. Kanno: Acta Mater. **49** (2001) 3981–3989.
4) K. Horikawa, S. Kuramoto and M. Kanno: Scr. Mater. **47** (2002) 131–135.
5) H. Okada and M. Kanno: Proc. of 4th Int. Conf. on Aluminum Alloys-Their Physical and Mechanical Properties, T. H. Sanders, Jr. and E. A. Starke, Jr., eds., Georgia Institute of Technology, Atlanta, GA (1994) pp. 314–321.
6) J. K. Tien, A. W. Thompson, I. M. Bernstein and R. J. Richards: Metall. Trans., A **7** (1976) 821–829.
7) J. A. Donovan: Metall. Trans. A **7** (1976) 1677–1683.
8) Y. Liang, P. Sofronis and N. Aravas: Acta Mater. **51** (2003) 2717–2730.
9) J. Lufrano and P. Sofronis: Acta Mater. **46** (1998) 1519–1526.
10) E. Sirois and H. K. Birnbaum: Acta Metall. **40** (1992) 1377–1385.
11) D. Shih, I. M. Robertson and H. K. Birnbaum: Acta Metall. **36** (1988) 111–124.
12) J. Ovejero Garcia, J. Mater. Sci. **20** (1985) 2623–2629.